Dishevelled (Dvl-2) activates canonical Wnt signalling in the absence of cytoplasmic puncta

Matthew J. Smalley[1], Nathalie Signoret[2], David Robertson[1], Alan Tilley[3], Anthony Hann [5], Ken Ewan[5], Yanning Ding[4], Hugh Paterson[4] and Trevor C. Dale[5,*]

[1]The Breakthrough Breast Cancer Research Centre, The Institute of Cancer Research, 237 Fulham Road, London, SW3 6JB, UK
[2]MRC Cell Biology Unit-LMCB, University College London, Gower Street, London, WC1E 6BT, UK
[3]Improvision, Viscount Centre II, University of Warwick Science Park, Milburn Hill Road, Coventry, CV4 7HS, UK
[4]CRC Centre for Cell and Molecular Biology, The Institute of Cancer Research, 237 Fulham Road, London, SW3 6JB, UK
[5]Cardiff School of Biosciences, Biomedical Sciences Building, Museum Avenue, Cardiff, CF10 3US, UK
*Author for correspondence (email: daletc@cardiff.ac.uk)

Accepted 15 August 2005
Journal of Cell Science 118, 5279-5289 Published by The Company of Biologists 2005
doi:10.1242/jcs.02647

Summary

Dishevelled family proteins are multidomain intracellular transducers of Wnt signals. Ectopically expressed mammalian Dishevelled 2 (Dvl-2) activates downstream signalling and localises to cytoplasmic puncta. It has been suggested that these Dvl-2-containing structures correspond to intracellular vesicles and may be involved in the Wnt signal transduction process. We report that cytoplasmic puncta are primarily formed in cells expressing Dvl-2 at high levels. Lower levels of expression can activate signalling without forming puncta. The structures do not localise with markers of the early or late endocytic pathway and time-lapse analysis demonstrates that Dvl-2 puncta move in a random fashion over short distances but do not originate from the plasma membrane. Based on our findings, we propose that Dvl-2 puncta are protein aggregates that are not required for signalling.

Supplementary material available online at
http://jcs.biologists.org/cgi/content/full/118/22/5279/DC1

Key words: Dishevelled, Dvl-2, endosomal, vesicle, Wnt

Introduction

Dishevelled family proteins (Dsh in *Drosophila*; XDsh in *Xenopus*; Dvl-1 to 3 in mammals) are key intracellular mediators of the Wnt signalling pathway. The current model of the canonical Wnt pathway (Bejsovec, 2005; Cong and Varmus, 2004; Moon, 2005a; Moon, 2005b; Smalley and Dale, 2001) suggests that, in the absence of a Wnt signal, the pivotal event in the pathway is the phosphorylation of β-catenin by the serine/threonine kinase glycogen synthase kinase-3β (GSK-3β). This phosphorylation occurs as part of a multiprotein complex including GSK-3β, casein kinase-1, the adenomatous polyposis coli (APC) protein, axin, protein phosphatase 2A (PP2A) and β-catenin. Phosphorylation targets β-catenin for ubiquitin-mediated degradation.

The Wnt signal is propagated following binding of the Wnt ligand to a heterodimeric complex consisting of a Frizzled receptor and an LDL-receptor-related protein (LRP) 5/6 protein (Cong et al., 2004; Tamai et al., 2000). This results in recruitment of axin to the LRP protein and Dishevelled to the Frizzled receptor (Cong et al., 2004; Mao et al., 2001; Tolwinski et al., 2003). In a manner not yet fully understood, this blocks the action of the β-catenin turnover complex, leading to β-catenin accumulation and interaction with T-cell factor (TCF) family transcription factors, enabling activation of transcription from promoters containing TCF binding sites.

The Frizzled receptors can potentially couple to two other downstream pathways, namely the planar cell polarity (PCP) pathway and the calcium-signalling pathway (Boutros and Mlodzik, 1999; Kuhl et al., 2000; Miller et al., 1999; Smalley and Dale, 2001). Dishevelled has been shown to function in both the PCP and canonical 'β-catenin' pathway. G-proteins may have a role in all three pathways (Bejsovec, 2005; Kuhl et al., 2000; Wu et al., 2005). The mechanisms underlying the role of Dishevelled in Wnt signalling have not yet been fully elucidated. However, several lines of evidence indicate that the cellular localization of Dsh may be important for its function in signal propagation.

Some ectopically expressed Frizzled family members can recruit Dishevelled to the plasma membrane (Axelrod et al., 1998; Cong et al., 2004) (M.S., unpublished data), and RNA interference studies have shown that Dishevelled is required for Frizzled activity in Frizzled/LRP receptor complexes but not for LRP function (Cong et al., 2004). Dishevelled is required to recruit axin to the Frizzled/LRP complex in a signal dependent manner (Cliffe et al., 2003; Cong et al., 2004). In addition, signalling via a Wnt5A/Frizzled4 combination down the PCP 'β-catenin-independent' pathway has been suggested to involve Dishevelled and a clathrin/β-arrestin2-dependent mechanism (Chen et al., 2003; Le Roy and Wrana, 2005). Lastly, Wingless signalling is downregulated via clathrin-mediated endocytosis of the Wingless protein into lysosomes (Dubois et al., 2001).

Dishevelled has three identified domains, namely an N-terminal DIX (for Dishevelled and axin proteins) domain, a central PDZ (for PSD-95, Discs-large and ZO-1 proteins) domain and a C-terminal DEP (for Dishevelled, EGL-10 and

Pleckstrin proteins) domain (Axelrod et al., 1998; Klingensmith et al., 1994; Sussman et al., 1994; Theisen et al., 1994). The DIX domain is thought to be required for the canonical (β-catenin) pathway (Moriguchi et al., 1999; Rothbacher et al., 2000) and mediates Dishevelled multimerisation and interaction with axin (Kishida et al., 1999). The DEP domain is thought to be required for PCP pathway signalling (Heisenberg et al., 2000; Li et al., 1999; Wallingford et al., 2000). The PDZ domain, on the other hand, may function in both pathways (Heisenberg et al., 2000; Moriguchi et al., 1999; Rothbacher et al., 2000; Wallingford et al., 2000).

Despite the uncertainty as to the mechanism of Dishevelled function, three findings are consistent across all studies of Dishevelled family proteins. First, ectopic expression of Dishevelled by transient transfection activates the canonical Wnt signalling pathway. There is, however, no evidence that this occurs via a physiological mechanism, although human DVL-1 has been reported as being overexpressed in breast tumours (Nagahata et al., 2003) and cervical squamous cell carcinoma (Okino et al., 2003). Secondly, immunostaining for ectopically expressed Dishevelled reveals that it is located in cytoplasmic puncta (Axelrod et al., 1998; Choi and Han, 2005; Cliffe et al., 2003; Fagotto et al., 1999; Smalley et al., 1999), which despite no direct evidence, have been described as vesicles (Capelluto et al., 2002; Torres and Nelson, 2000). Some authors have also argued that Dishevelled is additionally located at the actin cytoskeleton (Capelluto et al., 2002; Torres and Nelson, 2000) or microtubule network (Ciani et al., 2004; Krylova et al., 2000). Lastly, ectopic expression of Dishevelled and axin results in the colocalisation of these proteins (Fagotto et al., 1999; Smalley et al., 1999).

The nature of Dishevelled cytoplasmic puncta is unclear but it has been suggested that they are crucial for propagation of the Wnt signal (Capelluto et al., 2002; Choi and Han, 2005), possibly being the organelles in which cytoplasmic axin is transferred to the cell surface following activation of receptor complexes (Cliffe et al., 2003). Formation of Dishevelled puncta following ectopic expression has been shown to be dependent on the presence of the DIX domain. However, DIX domains have also been suggested to play a role in dimerisation/multimerisation.

In this study, we find that Dishevelled can localise with two distinct patterns whilst activating signalling. The distinct patterns of Dishevelled are differentially dependent on the DIX and PDZ domains, both of which are functionally required for signalling. We find that the DIX domain-dependent puncta are primarily formed at higher levels of expression, are not associated with endocytic vesicles, and probably represent protein aggregates.

Materials and Methods

Antibodies

High affinity rat anti-HA antibody 3F10 was obtained from Roche Diagnostics (Lewes, UK). Anti-γ-tubulin antibody was obtained from Sigma (Poole, UK). Antibodies to β-catenin, GSK-3β and early endosome antigen (EEA)-1 were obtained from BD Transduction Laboratories (Cowley, UK). Anti-human transferrin receptor antibody H68.2 was obtained from Zymed Laboratories (San Francisco, CA). Mouse anti-clathrin heavy chain antibody X22 was obtained from Cambridge Bioscience (Cambridge, UK). Rabbit anti-Dvl-2 antibody (Smalley et al., 1999), anti-hamster lysosomal glycoprotein Lgp-B antibody 3E9 (Signoret et al., 2000) and anti-primate CD63 antibody 1B5 (Fraile-Ramos et al., 2001) have been previously described.

Plasmids

HA-tagged Dvl-2 was previously described (Smalley et al., 1999). HA-Dvl-2-EGFP was made by subcloning the HA-Dvl-2 sequence from pcDNA3.1- (Invitrogen, Paisley, UK) into pEGFP-N3 (Clontech, Basingstoke, UK). HA-Dvl-2-estrogen receptor (ER) ligand-binding-domain fusion protein was made in two stages. First, residues 282-595 (SAGD to PATV) of the human estrogen receptor, were isolated from the EFG2ERP plasmid (a generous gift of Tariq Enver, Institute of Cancer Research, London, UK) by *Bst*EII and *Not*1 digestion and cloned into *Eco*RV/*Not*I-digested pcDNA 3.1+ (Invitrogen). This fragment of the ER cDNA also contained a G400V (HPVKL) mutation that reduced ER affinity for estradiol, thus preventing its activation by low levels of estradiol found in serum and tissue culture medium (data not shown). Next, HA-Dvl-2 was digested from HA-Dvl-2-EGFP using *Nhe*I and *Bam*HI. This fragment was then subcloned in-frame into the ER-pcDNA 3.1+ fusion plasmid cut with *Nhe*I/*Bam*HI. This resulted in the loss of the last 21 residues of Dvl-2 (starting with ASRQ) as well as the addition of a short linker sequence of 13 amino acids, derived from the multiple cloning site of the ER-pcDNA 3.1+ fusion plasmid, between the HA-Dvl-2 and the ER-ligand-binding domain. The protein was named HA-Dvl-2-ER. A similar approach was briefly mentioned elsewhere (Ding et al., 2000) but was not characterised in full.

The ΔDIX (lacking amino acids 61-156, from residues AGAK to SHEN) and ΔPDZ (lacking amino acids 324-404, from residues GDML to PAYP: equivalent to a *Xenopus* Dishevelled mutant (Xdd1) that is a dominant negative in both canonical and PCP signalling) (Heisenberg et al., 2000; Sokol, 1996; Wallingford et al., 2000) mutants were made by generating the mutations in the original HA-Dvl-2 construct and subsequently subcloning in the ER-fusion domain. The K446M HA-Dvl-2-ER plasmid was generated using a Quikchange site-directed mutagenesis kit (Stratagene, Amsterdam, The Netherlands) using the HA-Dvl-2-ER as the template DNA, according to the manufacturer's instructions with the following forward and reverse primers: 5′-GACCGCATGTGGCTCATGATCA-CCATCCCAAAC-3′ and 5′-GTTTGGGATGGTGATCATGAGCC-ACATGCGGTC-3′. The mutation (at residue 456 in the fusion protein) is equivalent to the Dsh^1 mutant of *Drosophila* Dishevelled, which shows planar polarity signalling defects in *Drosophila* (Boutros et al., 1998). The 'vesicle' and 'actin' mutants were generated following published methods (Capelluto et al., 2002) using the Quikchange kit with HA-Dvl-2-GFP. Diagrams of the constructs are represented in supplementary material Fig. S1. Human Frizzled 4 plasmid was a kind gift of Jeremy Nathans (HHMI, Chevy Chase, MD). The V5 epitope tag was added by standard PCR strategies.

Cell culture

Madin-Darby canine kidney (MDCK) cells and human embryonic kidney (HEK) 293 cells were obtained from ATCC (Rockville, Maryland, USA). HEK293 FLP-IN host cells were obtained from Invitrogen. All lines were maintained in Dulbecco's modified Eagle's medium (DMEM) containing 10% foetal calf serum at 37°C in 5% CO_2. Medium for HEK293 FLP-IN Host cells was supplemented with 0.25 mg/ml zeocin (Invitrogen).

DHFR-deficient Chinese hamster ovary (CHO) cells expressing the human transferrin receptor were maintained in nucleoside-free aMEM supplemented with Glutamax and 10% foetal calf serum (FCS) and 1 mg/ml G418, as previously described (Signoret et al., 2005).

For preparation of Wnt3a-conditioned medium, CRL-2647 Wnt3a-expressing mouse L-cells (LGC Promochem, Teddington, UK) were routinely cultured in DMEM medium supplemented with 0.4 mg/ml

G418 (Invitrogen, Paisley, UK). Cells were passaged at a 1:10 split ratio and grown for 4 days before collection and 0.22 μm filtration of conditioned medium. Activity of Wnt3a-conditioned medium was tested by exposing mouse L-cells to 50% Wnt3a-conditioned medium for 8 hours. Extracts were made in RIPA buffer supplemented with complete protease inhibitor tablets (Roche, Lewes, UK) and analysed by SDS-PAGE. Blots were probed for β-catenin accumulation. Active Wnt3a-conditioned medium, but not control medium, could induce β-catenin accumulation within 8 hours.

Microinjection

Groups of subconfluent MDCK cells cultured on 50 mm MatTek glass-bottomed Petri dishes were microinjected in the nucleus with HA-Dvl-2-EGFP plasmid diluted to 25 μg/ml in PBS. After a 6 hour expression period, the HA-Dvl-2-EGFP expressing cells were imaged using a ×40 Plan-Apo objective mounted on a Nikon TE2000 inverted fluorescence microscope with incubator jacket and CO_2 control, linked to a Nikon CI confocal imaging system. Time-lapse movie sequences were assembled, using Nikon EZC1 software, from confocal images of GFP-fluorescing cells acquired at 1 minute intervals, and subsequently converted into 12-frame-per-second 'avi' files.

Movies were analysed using Adobe Premier Pro 1.5. They were slowed down to 30% of their original speed for easier analysis of the patterns of movement of the Dvl-2 puncta. One movie (supplementary material Movie 1A) showed good detail of one cell which ectopically expressed Dvl-2-EGFP at high levels and one cell which expressed it at lower levels. The software was used to zoom in on these cells and generate separate avi movies of these two magnified regions. In addition, a small number of frames from these regions were captured and saved as bmp files to generate a time series of stills. These stills were imported into Adobe Photoshop 7.0 and composite figures generated. The composites were then examined in parallel with a frame-by-frame viewing of the movies in Premier Pro to allow individual vesicles to be false coloured. This enabled easier illustration of the representative patterns of movement of the puncta.

Establishment of stable cell lines

Cell lines that stably expressed fusion proteins were established using the Invitrogen 'FLP-In' system. This uses a HEK293-based host cell line containing a single copy of a β-galactosidase gene and a zeocin-resistance gene in a cassette flanked by FLP-recombinase recognition (FRT) sites. The cassette is inserted in a site of known transcriptional activity in the cells, as determined by β-galactosidase activity and zeocin resistance.

To establish the cell lines, the HA-Dvl-2-ER wild-type and mutant fusion proteins were subcloned by *Nhe*I/*Pme*I digest into plasmid pcDNA5/FRT. Transfections and selections were performed according to manufacturer's recommendations. Cells in which FLP recombinase insertion has been successful gain a single copy of the HA-Dvl-2-ER hygromycin-resistance cassette, lose β-galactosidase activity and become zeocin sensitive. The cultures were selected in hygromycin (0.2 mg/ml) for positive clones. Each transfection resulted in 20-40 clones growing after hygromycin selection. As the HEK293 host cell line has a clonal insertion site, HA-Dvl-2-ER insertions were expected to be identical and the clones were therefore pooled to produce a 'polyclonal line'. Subsequent analysis confirmed that there was little variation in levels of HA-Dvl-2-ER expression.

Luciferase assay for transcriptional activation

Luciferase reporter assays were essentially carried out as described (Smalley et al., 1999) using TOPFLASH or FOPFLASH (Korinek et al., 1997) reporters for analysis of TCF-dependent (i.e. β-catenin pathway) transcription. A CMV promoter-driven β-galactosidase plasmid was used as a marker of transfection efficiency. Cell lysates were analysed for luciferase and β-galactosidase activity and for levels of transfected proteins from the detergent soluble and insoluble fraction obtained during cell lysis.

Protein analysis and western blotting

For protein analysis in stable cell lines, cells were cultured to 80-90% confluence in 100 mm diameter dishes, re-fed with medium containing 1 μM estradiol or with ethanol vehicle only (control) medium and harvested at varying times as described. Cells were harvested by either of two methods. Total cell lysates were prepared by scraping into 2× SDS loading buffer, shearing through blunt needles and SDS-PAGE analysis. Detergent-soluble and -insoluble extracts were prepared by scraping cells into 1 ml per dish of ice-cold lysis buffer (1% NP40, 1 mM Tris-HCl pH 7.4, 150 mM NaCl, 5 mM EDTA, 1 mM DTT, 100 nM okadaic acid and 1:100 Sigma mammalian cell protease inhibitors). Following a 20 minute incubation, lysates were spun at 17,949 ***g*** for 20 minutes and samples were normalised for protein levels. Detergent-insoluble fractions were normalised to their respective soluble fraction based on equivalent fractions of cellular material (i.e. if 1/100 of the soluble material was loaded then 1/100 of the insoluble material was also loaded). Insoluble material was taken up directly into 2× SDS loading buffer and then sheared. Samples were blotted on to nitrocellulose and probed by standard procedures. HRP-conjugated secondary antibodies were obtained from Amersham Pharmacia Biotech (Little Chalfont, UK) and Sigma.

The protocol for the equilibrium flotation sucrose gradient to assess membrane association was based on Spearman et al. (Spearman et al., 1997) as modified by others (Ono and Freed, 1999; Swanson and Hoppe, 2004). For this procedure, CHO cells were nucleofected with HA-Dvl-2-GFP. After 36 hours, transfection efficiency was estimated from the number of GFP positive cells. The cells were detached in PBS/10 mM EDTA, pelleted at 1000 ***g***, and resuspended in 300 μl NTE (10 mM Tris-HCl; 1 mM EDTA; 10% w/v sucrose; Roche mini-cocktail protease inhibitors) and then sonicated twice on ice for 15 seconds. Following centrifugation at 1000 ***g***, 250 μl post nuclear supernatant was mixed with 1.25 ml of 85.5% w/v sucrose in TE (10 mM Tris-HCl, 1 mM EDTA). This mix was placed at the bottom of an ultracentrifuge tube, overlayed with 7 ml of 65% sucrose (w/v) in TE followed by 3.25 ml NTE and then spun at 100,000 ***g*** for 18 hours at 4°C in a swing-out rotor (Beckmann Coulter, Bucks, UK). Twelve 1 ml fractions were collected by hand from the top of the sample and gradient linearity was checked by measuring the refractive index of each fraction using a refractometer. NP40 was added to each fraction to a final concentration of 1% and they were incubated on ice for 30 minutes. 15 μl of each fraction was analysed by SDS-PAGE and western blotting for transferrin receptor, clathrin heavy chain and HA-Dvl-2-GFP.

Confocal immunofluorescence analysis

For immunofluorescence analysis of transiently transfected cells, MDCK and HEK 293 cells were cultured on glass coverslips and transfected using Effectene Reagent (Qiagen, Crawley, UK) according to the manufacturer's instructions. After overnight incubation, cultures were re-fed with medium containing 1 μM β-estradiol or control medium for varying incubation periods, fixed in 4% paraformaldehyde in PBS for 15 minutes and then permeabilised with 0.02% Triton X-100 in PBS for 10 minutes. For stable cell lines, cells were grown on glass coverslips, re-fed with medium containing 1 μM estradiol or with control medium and fixed, after varying incubation periods, in 4% paraformaldehyde. For γ-tubulin staining cultures were fixed in ice-cold methanol for 3 minutes. The staining protocol was essentially as described (Smalley et al., 1998). Fluorescently labelled secondary antibodies used were anti-rat Alexa-488 and anti-mouse

Alexa-568 (Molecular Probes, Invitrogen, Paisley, UK). Where indicated, nuclei were visualised using ToPro III dye (Molecular Probes).

For colocalization experiments with endosomal markers in CHO cells, HA-Dvl-2-GFP proteins were transiently expressed using nucleofection (Amaxa, Köln, Germany). Transfected cells were seeded on coverslips and immunofluorescence patterns analysed 40 hours post-nucleofection. Cells were fixed in 3% paraformaldehyde for 15 minutes at room temperature, and free aldehyde groups quenched with 50 mM NH_4Cl in PBS. Fixed and quenched samples were permeabilised in PBS with 0.2% gelatin (PBS/gelatin) containing 0.05% saponin, before being stained by indirect immunofluorescence using Alexa-594-conjugated goat anti-mouse (1:1000; Molecular Probes) to detect the primary antibody. Cells were washed in PBS/gelatin, then in PBS and mounted in medium containing Mowiol as described (Signoret and Marsh, 2000).

For transferrin uptake in CHO cells, cells were incubated in binding medium (BM: RPMI 1640 without bicarbonate containing 0.2% BSA and 10 mM HEPES, pH 7.0) then treated with 200 nM Alexa-594-conjugated transferrin (^{594}Tf) in 37°C BM for 60 minutes, before being fixed and quenched.

Coverslips were examined using a Zeiss Axioskop microscope, Leica TCS NT or a Nikon Optiphot-2 microscope equipped with an MRC BioRad 1024 confocal laser scanner. In all cases, multicolour images were collected sequentially and processed using Adobe Photoshop software. Note that isotype-matched non-specific control primary antibodies gave little or no background staining.

3D time-lapse imaging

HEK293 cells transiently transfected with HA-Dvl-2-EGFP were imaged on a Zeiss Axiovert 200M with a 63× oil immersion lens (numerical aperture 1.4) with a Zeiss filter set 10 and an EXFO Photonics X-CITE 120 fluorescence microscope illumination system. Images were collected with a Hamamtsu Orca AG camera (binning 2×2). The system was controlled by the Improvision Volocity 3DM acquisition system on an Apple Mac 1.8 dual processor. Optical slices were generated by Optigrid Structural Light Imaging System (for confocal quality 3D). The system was used in combination with a Vistek 300 anti-vibration platform and an Applied Scientific Instrumentation PZM2000 Piezo Z microstepper (Improvision, Coventry, UK).

Data was collected over 17 time-points. At each time-point, a stack of 45 images was collected, each with a duration of approximately 34 seconds. At the end of the collection of one time point stack, the next was immediately collected. Thus, each time point was 34 seconds apart. For each HA-Dvl-2-EGFP body analysed, a velocity was determined. For each body with three or more data points available, a 'meandering index' was calculated. This is defined as the displacement (the straight line distance from start to end point) divided by the total track length (i.e. the actual distance travelled by each body). A meandering index of 1 would therefore indicate directional transport.

Immunoelectron microscopy

Low-temperature embedding with Lowicryl HM20 was essentially as published (Carlemalm et al., 1982). The cell pellet from the transfected HEK293 cells was embedded in 3% agar and fixed for 1 hour at 4°C in a mixture of 0.25% glutaraldehyde and 0.25% osmium tetroxide buffered with 0.1 M phosphate at pH 7.4. Following fixation, the sample was washed in the same buffer for 30 minutes and dehydrated for 15 minutes in 30% ethanol at 4°C before being transferred into an automated freeze-substitution chamber (Reichert AFS, Leica, UK). Progressive lowering of the temperature for resin embedding was conducted (Carlemalm et al., 1982) with the following modifications: –15°C in 55% ethanol for 30 minutes; –20°C in 70% ethanol for 1 hour; –25°C in 90% ethanol for 1 hour; –25°C in 1:1 mixture of 90% ethanol and Lowicryl HM 20 for 1 hour, –25°C in 1:2 90% ethanol/Lowicryl for 1 hour, –25°C in neat Lowicryl overnight and –25°C in fresh Lowicryl under UV light for 48 hours.

Post-embedding immunogold labelling

Ultrathin sections (90 nm) from Lowicryl-embedded blocks were incubated for 1 hour on drops of blocking solution containing 0.2 M phosphate-buffered saline (pH 7.8) and 0.2% BSA. The primary (1:100 dilution) and secondary antibodies (1:20 dilution) were also prepared in this solution. The sections were incubated in primary antibody overnight at 4°C. After washing with the same blocking solution, the sections were incubated for 2 hours at 20°C with mouse anti-rat IgG conjugated with 10 nm gold. Sections were briefly washed with PBS followed by several rinses in double-distilled water and then counterstained with lead citrate for 5 minutes before examination in a Philips EM 308 transmission electron microscope.

Results

High-level and low-level expression of Dvl-2 results in two distinct localisation patterns

To investigate the punctate nature of dishevelled localisation, HA-epitope tagged Dvl-2 fusion proteins were expressed using both transient and stable systems. HA-tagged Dvl-2 was fused at the C-terminus to either GFP (HA-Dvl-2-EGFP) or to an estrogen-inducible Dvl-2 fusion protein (HA-Dvl-2-ER; a schematic representation of the proteins is shown in supplementary material Fig. S1). Following transient transfection into HEK293, MDCK and CHO cells the characteristic pattern of punctate structures previously observed for HA-Dvl-2 was observed in untreated HA-Dvl-2-EGFP-expressing cells and in HA-Dvl-2-ER-expressing cells following estrogen induction (Fig. 1) (Axelrod et al., 1998; Choi and Han, 2005; Cliffe et al., 2003; Fagotto et al., 1999;

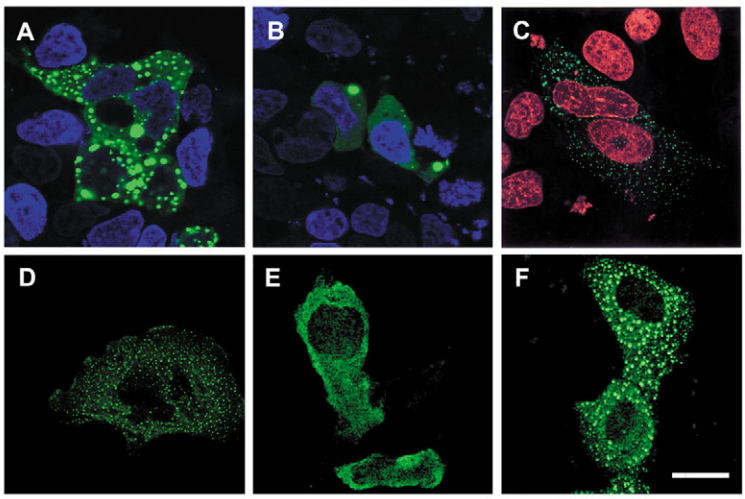

Fig. 1. Localisation of ectopically expressed Dvl-2. (A-D) Localisation of transiently expressed HA-Dvl-2-EGFP (green) in HEK293 cells (A-B, nuclei counterstained with ToPro III), MDCK cells (C, nuclei counterstained with ToPro III) and CHO cells (D, no nuclear counterstain). (E-F) Localisation of transiently expressed HA-Dvl-2-ER (green) in MDCK cells. Cells were fixed 1 hour after re-feeding with medium containing ethanol vehicle (E) or 1 μM β-estradiol (F). Bar, 15 μm.

Smalley et al., 1999; Torres and Nelson, 2000). This agreed with our previous observations and suggested that the method of production of active Dishevelled protein (translational accumulation or estrogen activation) was independent of the nature of the structures generated. Secondly, the HA-Dvl-2-ER protein was stably expressed from a single-copy integration site in HEK293 cells (Fig. 2). Long-term expression of non-inducible forms of Dvl-2 could not be achieved, suggesting that this reduces cell viability. Expression of the inducible HA-Dvl-2-ER protein in the HEK293 cell line was at levels close to that of endogenous Dvl-2 levels (near physiological) (Fig. 3). By contrast with cells transiently expressing HA-Dvl-2-ER, treatment of the single copy cell line (HEK293-HA-Dvl2-ER) with β-estradiol for 60 minutes resulted in a different HA staining pattern consisting of a single large fluorescent mass near the nucleus together with juxtamembrane staining in the region of the cortical actin cytoskeleton (Fig. 2A-C; supplementary material Fig. S3). Co-staining with an anti-γ-tubulin antibody established that the large fluorescent mass near the nucleus corresponded to the microtubule organising centre (MTOC) (Fig. 2D-F). Localisation of HA-Dvl-2-ER protein to the MTOC was insensitive to nocodazole but nocodazole treatment did disrupt the juxtamembrane localisation of the protein (Fig. 2G-I) suggesting that this was microtubule-dependent.

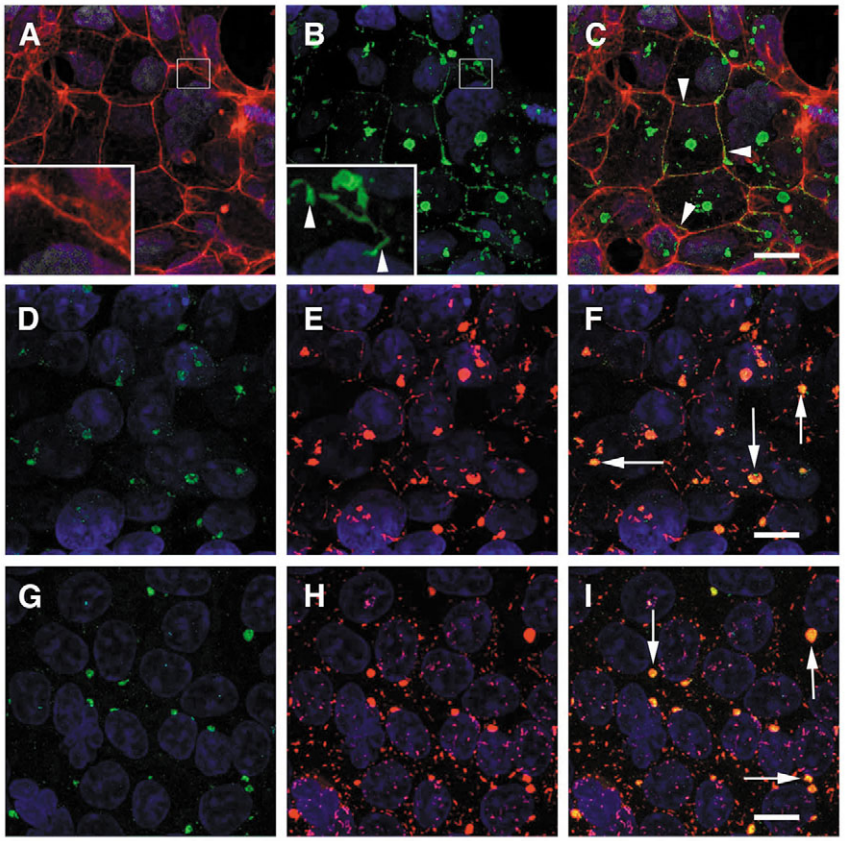

Fig. 2. Localisation of activated HA-Dvl-2-ER protein in single-copy cell line. All images represent a projection of a series of stacked optical sections. Nuclei were stained with ToPro III (blue). Areas of colocalisation in overlaid images appear yellow. Cultures were treated with 1 μM β-estradiol for 1 hour, fixed and stained, except as noted for panels G-I. (A-C) Colocalisation of F-actin and HA-Dvl-2-ER. F-actin is in red (A) and HA-Dvl-2-ER in green (B). Arrowheads in inset image indicate patches of HA staining projecting from the juxtamembrane region into cell interior. Arrowheads in the merged image (C) indicate examples of areas of colocalisation at the cell membrane. The complete series of optical sections is shown in supplementary material Fig. S3. (D-F) Colocalisation of γ-tubulin and HA-Dvl-2-ER protein with γ-tubulin in green (D) and HA-Dvl-2-ER in red (E). Arrows in merged image (F) indicate examples of co-staining at MTOC. (G-I) Disruption of membrane localisation of HA-Dvl2-ER protein by nocodazole treatment. Cells were treated with 33 μM nocodazole (a concentration which disrupts microtubule networks but not the MTOC) in DMSO for 3 hours and then with 1 μM β-estradiol plus nocodazole for up to 1 hour. γ-tubulin is in green (G) and HA-Dvl-2-ER in red (H). Arrows in merged image (I) indicate examples of co-staining at MTOC. Staining of control coverslips with an anti-α-tubulin antibody confirmed that microtubule networks were disrupted only in nocodazole-treated cultures and were not affected by the fixation protocol (data not shown). Similar disruption of HA-Dvl-2-ER at the membrane was seen in cells treated with nocodazole for periods of between 2 hours and 15 minutes (data not shown). Bars, 10 μm.

We examined the ability of Dvl-2 to activate the canonical Wnt signalling pathway in both the high-level and low-level expression systems. The results (Fig. 3) showed that ligand-dependent activation of HA-Dvl-2-ER stimulated this pathway in both systems. Thus, activation of canonical Wnt signalling can be demonstrated under conditions involving two very different Dvl-2 localisation patterns.

Dvl-2 puncta do not colocalise with endocytic markers

To further investigate the nature of the predominant punctate staining pattern observed following transient ectopic expression, we studied its relationship to the cellular endocytic pathway as a role for endocytosis in Wnt signalling has been recently proposed (Chen et al., 2003; Cliffe et al., 2003; Dubois et al., 2001; Le Roy and Wrana, 2005). HA-Dvl-2-EGFP-transfected HEK293 cells were co-stained for EEA-1 (early/sorting endosome), CD63 (labelling late endosomes and lysosomes) and the transferrin receptor (mainly found in early/sorting endosome and recycling endosomes; Fig. 4A-F). We also fed HA-Dvl-2-EGFP-transfected CHO cells with Alexa-594-coupled transferrin to label the early endocytic pathway from clathrin-coated pits to recycling endosomes (Fig. 4G,H) or co-stained these cells for LgpB, a marker of late endosomal structures (Fig. 4I). In these experiments, there was no detectable overlap of HA-Dvl-2-EGFP with any of the endosomal markers tested in either cell type. Thus, cytoplasmic Dvl-2 puncta do not correspond to clathrin-coated vesicles, early and recycling endosomes, or late endosomes and lysosomes. Interestingly, the presence of very large Dishevelled-containing structures in some transfected cells did not affect the distribution or appearance of the endosomal compartments, suggesting that the two sets of

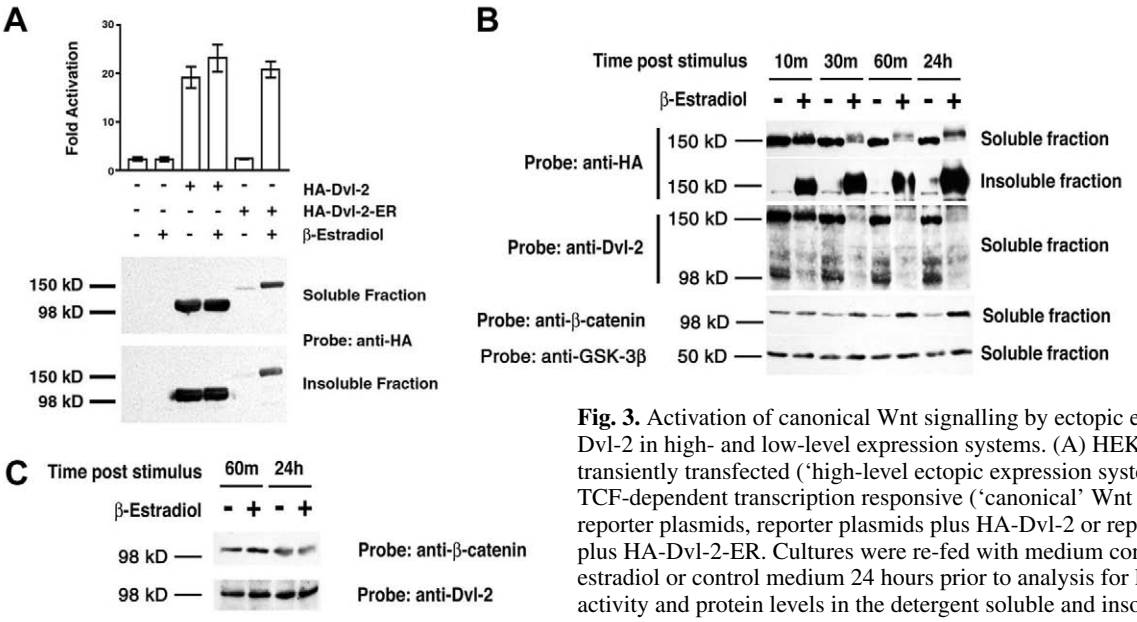

Fig. 3. Activation of canonical Wnt signalling by ectopic expression of Dvl-2 in high- and low-level expression systems. (A) HEK293 cells were transiently transfected ('high-level ectopic expression system') with either TCF-dependent transcription responsive ('canonical' Wnt signalling) reporter plasmids, reporter plasmids plus HA-Dvl-2 or reporter plasmids plus HA-Dvl-2-ER. Cultures were re-fed with medium containing 1 μM estradiol or control medium 24 hours prior to analysis for luciferase activity and protein levels in the detergent soluble and insoluble fractions of the cell extracts. (B) Time course of activation of canonical Wnt signalling pathway in Dvl-2-ER single-copy cell line. The cells were re-fed with medium containing 1 μM estradiol or with control medium and then harvested after 10, 30 and 60 minutes (10m/30m/60m) and 24 hours (24h) of induction. Detergent-soluble and -insoluble fractions were analysed by SDS-PAGE and western blotting. Identical protein levels were run on the gels. Blots were probed for the HA-tagged exogenous Dishevelled, for endogenous and exogenous Dvl-2 with a rabbit polyclonal anti-Dvl-2 and for endogenous β-catenin and GSK-3β. Note that although GSK-3β levels remain constant, there was an increase in soluble β-catenin levels from 30 minutes after β-estradiol treatment. Also, note the disappearance of the endogenous Dvl-2 protein (anti-Dvl-2 probe, 98kD band) from the soluble fraction following β-estradiol treatment, paralleling that of the single-copy fusion protein (150 kDa band). Finally, note the similarity in expression levels of the endogenous and exogenous proteins (estimated at three- to fivefold higher for the fusion protein). (C) Analysis of β-catenin and endogenous Dvl-2 expression in the parental cell line after 60 minutes (60m) and 24 hours (24h) of β-estradiol treatment. Note that there was no change in expression levels.

structures are independent. It is therefore unlikely that the predominant punctate staining pattern results from Dvl-2 internalisation and endocytic transport.

We used thawed low-temperature-embedding immunoelectron microscopy, which allows immunolocalisation of proteins as well as visualisation of ultrastructural features such as membranes, to determine if cytoplasmic Dvl-2 puncta were membrane-bound. We detected nuclear membranes, as well as membranes around mitochondria (Fig. 4J) and other organelles (data not shown), but we saw no evidence of membrane around the electron-dense, immuno-gold-labelled Dvl-2 puncta.

Domain dependence of intracellular distribution following transient expression

It has been reported that the formation of puncta requires the DIX but not the PDZ or DEP domains (Capelluto et al., 2002). However, both the DIX and PDZ domains are required for canonical Wnt signalling (Moriguchi et al., 1999; Rothbacher et al., 2000) whereas the *Dsh*^{l} mutation in the DEP domain does not affect the canonical pathway (Boutros et al., 1998; Moriguchi et al., 1999).

To examine the domain dependence of the HA-Dvl-2-ER protein localisation, a range of mutant constructs were transiently expressed in MDCK cells (Fig. 5A-F). In contrast to the wild-type protein (compare with Fig. 1E,F), the ΔDIX mutant protein did not form punctate structures following estradiol treatment, whereas the ΔPDZ and K446M-DEP domain mutant formed punctate structures similar to the wild-type protein (Fig. 5D,F). This confirmed previous studies showing that the formation of the puncta was dependent upon the DIX domain, but independent of the PDZ and K446M-DEP domains. The data further confirmed that the HA-Dvl-2-ER fusion protein expression pattern was representative of that of the HA-Dvl-2 wild-type protein.

Analysis of the ability of the wild-type and mutant proteins to activate the canonical Wnt signalling pathway (using the Topflash reporter assay) (Korinek et al., 1997; Smalley et al., 1999) demonstrated that although the K446M mutant behaved identically to the wild-type protein upon activation with β-estradiol, the ΔDIX protein failed to activate TCF-dependent transcription and the ΔPDZ protein only retained minimal activity upon addition of β-estradiol (supplementary material Fig. S2). This confirms previous reports and demonstrates that the ER domain does not interfere with the 'normal' behaviour of this protein.

Point mutations within the DIX domain were proposed to alter 'vesicle' (K68A / E69A) or actin (K58A) association (Capelluto et al., 2002). These point mutations were introduced into the Dvl-2-EGFP expression constructs which were then transfected into HEK293 cells (Fig. 5G-J). With both HA-Dvl-2-EGFP K58A (Fig. 5H) and HA-Dvl-2-EGFP K68A E69A (Fig. 5I,J) puncta were still observed, despite the mutations, although overall HA-Dvl-2-EGFP K68A E69A had a stronger, more diffuse background stain and tended to give

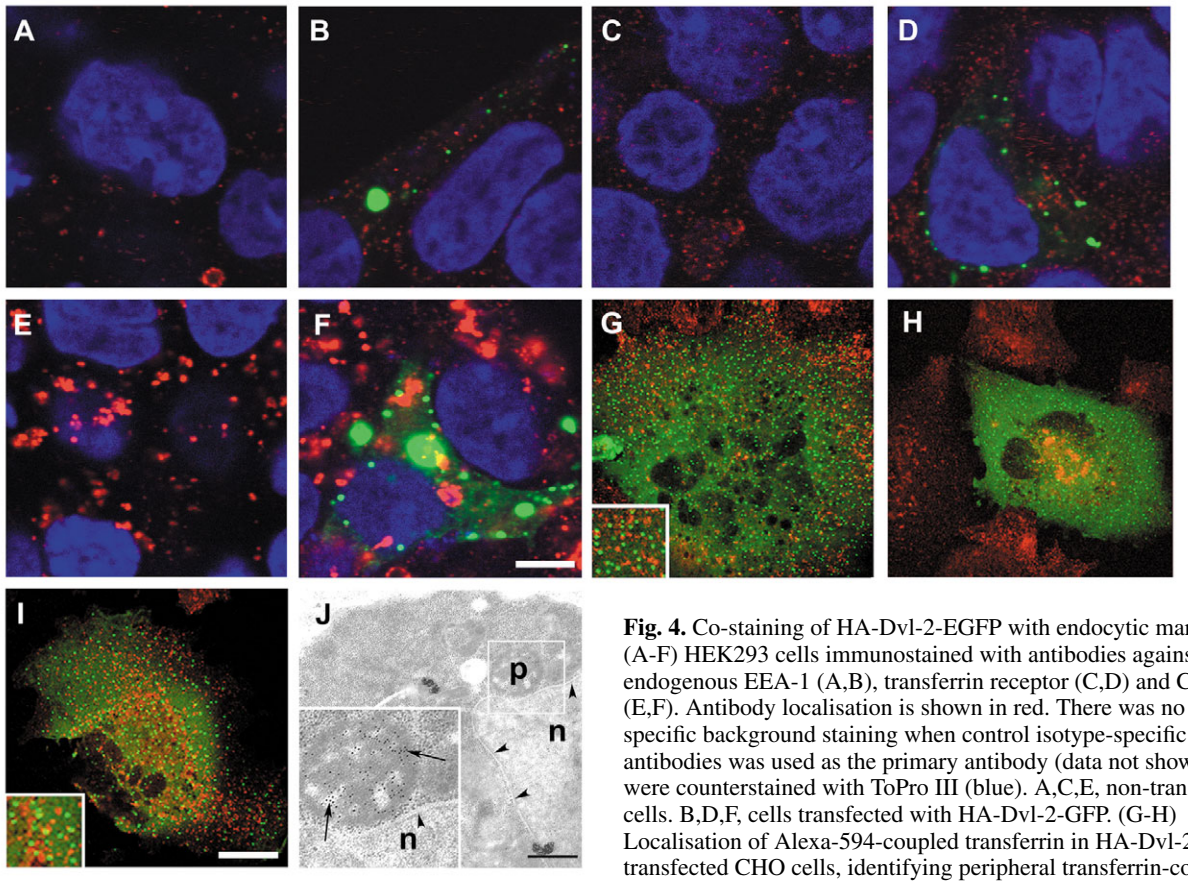

Fig. 4. Co-staining of HA-Dvl-2-EGFP with endocytic markers. (A-F) HEK293 cells immunostained with antibodies against endogenous EEA-1 (A,B), transferrin receptor (C,D) and CD63 (E,F). Antibody localisation is shown in red. There was no non-specific background staining when control isotype-specific antibodies was used as the primary antibody (data not shown). Nuclei were counterstained with ToPro III (blue). A,C,E, non-transfected cells. B,D,F, cells transfected with HA-Dvl-2-GFP. (G-H) Localisation of Alexa-594-coupled transferrin in HA-Dvl-2-GFP-transfected CHO cells, identifying peripheral transferrin-containing vesicles and early endosomes (G) or perinuclear recycling endosomes (H). (I) Localisation of late endosomes in HA-Dvl-2-GFP transfected CHO cells using an antibody to LgpB. Note that HA-Dvl-2-GFP failed to colocalise with any of these markers. (J) Analysis of HA-Dvl-2-GFP puncta using electron microscopy of HA-Dvl-2-GFP transfected HEK293 cells. The nuclear membrane (arrowheads) is clearly seen around the nucleus (n). In contrast, there is no evidence of a membrane around the electron-dense body (p), in which the HA-Dvl-2-GFP is concentrated, as shown by the anti-HA immuno-gold labelling in the magnified inset box (arrows). Bars, 5 μm (A-F); 20 μm (G-I); 1 μm (J).

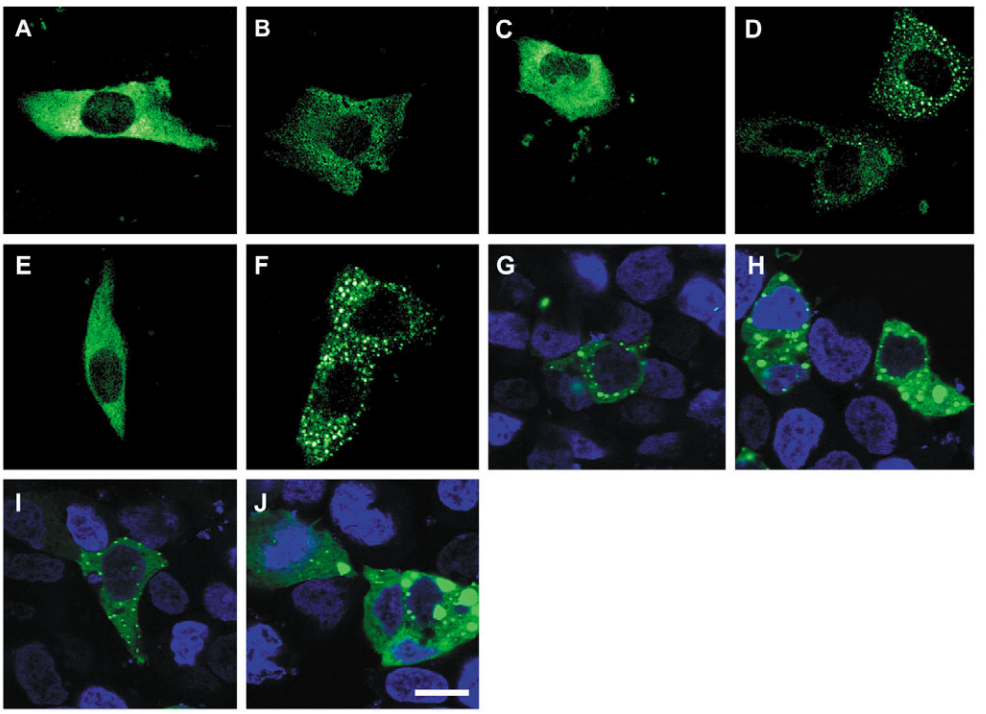

Fig. 5. Domain dependence of Dvl-2 localisation in transient ectopic expression systems. (A-F) Immunolocalisation of HA-Dvl-2-ER proteins transiently transfected into MDCK cells. Cells were fixed 1 hour after re-feeding with medium containing 1 μM β-estradiol or ethanol vehicle. (A) ΔDIX HA-Dvl-2-ER vehicle only. (B) ΔDIX HA-Dvl-2-ER treated with 1 μM estradiol. (C) ΔPDZ HA-Dvl-2-ER vehicle only. (D) ΔPDZ HA-Dvl-2-ER treated with 1 μM estradiol. (E) K446M HA-Dvl-2-ER vehicle only. (F) K446M HA-Dvl-2-ER treated with 1 μM estradiol. (G-J) Staining pattern of 'actin mutant' and 'vesicle mutant' Dvl-2 transfected into HEK293 cells. Dvl-2 localisation is in green and nuclei were counterstained with ToPro III (blue). (G) Wild-type HA-Dvl-2-EGFP. (H) HA-Dvl-2-EGFP K58A. (I,J) HA-Dvl-2-EGFP K68A,E69A. Bar, 8 μm.

rise to fewer puncta. Furthermore, we never observed colocalisation of ectopically expressed Dvl-2 with actin stress fibres.

Localisation of Dvl-2 to the MTOC and juxtamembrane region at low expression levels is dependent on the PDZ domain

Time-course analyses in the single copy cell line showed that as little as 30 minutes of estrogen induction could lead to β-catenin accumulation. Accumulation of β-catenin did not occur in similarly treated parental cells (Fig. 3). The estrogen-dependent induction of β-catenin by Dishevelled in the single-copy cell line argues that the puncta seen in high-level overexpressing cells (Fig. 1F) were not required for Wnt signalling. To examine the domain-dependence of Dvl-2 localisation in the single copy cell line, we generated additional single-copy cell lines expressing the ΔDIX, ΔPDZ and K446M-DEP mutants and examined the localisation of the HA-tagged protein 60 minutes after addition of estradiol (Fig. 6). Remarkably, both the ΔDIX and K446M-DEP domain variants had essentially identical staining patterns to that of the wild-type protein. Slightly higher levels of cytosolic staining remained following estrogen induction for both DIX and DEP domain mutants. However, loss of the PDZ domain completely abolished the MTOC and cell membrane localisation.

Thus, the domain dependency of localisation, as well as the pattern of localisation of the HA-Dvl-2-ER protein, is different depending upon whether it is expressed at high or very low levels. As the localisation and domain dependencies of inducible HA-Dvl-2-ER and constitutively active HA-Dvl-2-EGFP are identical at high levels of ectopic expression, this suggests that expression levels are the most important determinant of the localisation of exogenously expressed Dvl-2. Interestingly, those cells transiently expressing low levels of HA-Dvl-2-ER showed a similar pattern to that observed in the single-copy cell line (data not shown). Thus at high levels of expression, the punctate distribution is dependent on the presence of the DIX domains whereas at lower (near physiological levels), the patterns of localisation were dependent on the PDZ domain.

Dishevelled localisation may also be dependent upon its association with Frizzled proteins (Cong et al., 2004). We therefore examined the effects of coexpression of V5-epitope-tagged Frizzled-4 with HA-Dvl-2-ER. The results (supplementary material Fig. S4) demonstrated that coexpression relocalised HA-Dvl-2-ER to the plasma membrane. This occurred whether or not β-estradiol was added suggesting that conditional activation of Dishevelled is overcome when both HA-Dvl-2-ER and Frizzled are overexpressed.

Time-lapse microscopy analysis of Dvl-2 cellular distribution

To examine the distribution of Dvl-2 puncta over time, we carried out time-lapse fluorescence microscopy analysis of the localisation of HA-Dvl-2-EGFP microinjected into MDCK cells. The data are presented in the supplementary material Movies 1A-C and in Fig. 7. We observed cells with large bright fluorescent masses (Movie 1B and Fig. 7A) and smaller cytoplasmic puncta (Movie 1C and Fig. 7B). The puncta did not move in a coordinated fashion or over long distances within the cytoplasm. Instead, they were localised in a restricted area and appeared to oscillate back and forth (see the marked bodies in Fig. 7). Occasionally the structures merged with each other to make progressively larger cytoplasmic structures, suggesting that the larger bodies are derived from fusion of smaller structures, as in the case of the bodies marked red and orange in Fig. 7.

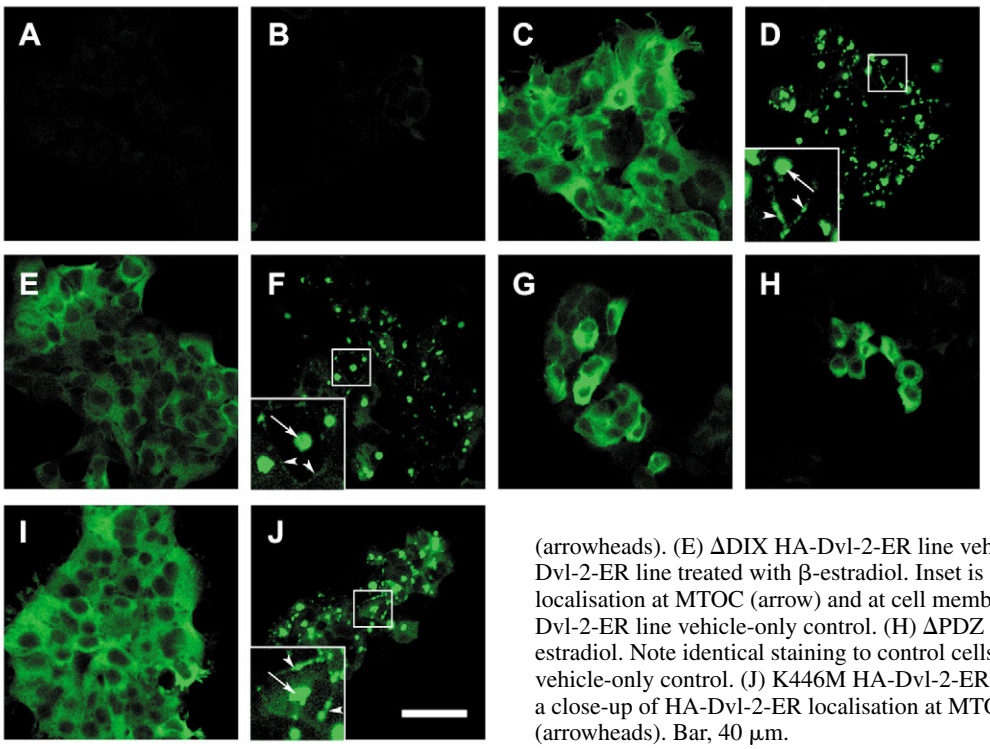

Fig. 6. Domain dependence of Dvl-2-ER localisation in single-copy cell lines. All panels were stained with anti-HA antibody. (A) Parental HEK293 cells treated with vehicle only for 1 hour. (B) Parental HEK293 cells treated with 1 μM β-estradiol for 1 hour. (C) Wild-type HA-Dvl-2-ER line vehicle-only control. (D) Wild-type HA-Dvl-2-ER line treated with 1 μM β-estradiol for 1 hour. Inset is a close-up of HA-Dvl-2-ER localisation at MTOC (arrow) and at cell membranes (arrowheads). (E) ΔDIX HA-Dvl-2-ER line vehicle-only control. (F) ΔDIX HA-Dvl-2-ER line treated with β-estradiol. Inset is a close-up of HA-Dvl-2-ER localisation at MTOC (arrow) and at cell membranes (arrowheads). (G) ΔPDZ HA-Dvl-2-ER line vehicle-only control. (H) ΔPDZ HA-Dvl-2-ER line treated with β-estradiol. Note identical staining to control cells. (I) K446M HA-Dvl-2-ER line vehicle-only control. (J) K446M HA-Dvl-2-ER line treated with β-estradiol. Inset is a close-up of HA-Dvl-2-ER localisation at MTOC (arrow) and at cell membranes (arrowheads). Bar, 40 μm.

We also used 3D fluorescence time-lapse image analysis with the Improvision Volocity 3DM System to analyse the movement of the smaller puncta. HA-Dvl-2-GFP was transiently ectopically expressed in HEK293 cells and data collected on the behaviour of 104 of the smaller puncta (rather than the large aggregates) (supplementary material Movies 2A,B and Table S1). The measurements indicated that they travelled at 0.024±0.01 μm/second, with a meandering index of around 0.5, suggesting that the movement was random, rather than directional.

Finally, we examined whether the movement of Dvl-2 puncta changed in response to a Wnt signal. HEK293 cells were transfected with HA-Dvl-2-GFP and treated with Wnt-3A conditioned medium or control medium for a 2 hour period. The movement of Dvl-2 puncta over this period was recorded by time-lapse video microscopy. Analysis of the data demonstrated that there was no difference between the random movements of the puncta in the control cultures compared to that in the cultures treated with Wnt-3A-conditioned media (data not shown).

Equilibrium flotation centrifugation analysis of Dvl-2 cellular distribution

In order to establish whether the HA-Dvl-2-GFP puncta may correspond to cytoplasmic aggregates resulting from the multimerization of ectopically expressed protein, we performed equilibrium flotation centrifugation (Ono and Freed, 1999; Spearman et al., 1997; Swanson and Hoppe, 2004) (supplementary material Fig. S5). In this assay, nuclei-free cell lysates are layered at the bottom of a sucrose step gradient and centrifuged to equilibrium. Cellular membranes rise to the high-low sucrose interface (fractions 4-6 as determined by refractive index measurement) where membrane-associated proteins are readily identified when fractions are collected and analysed (e.g. transferrin receptor and clathrin), whereas protein aggregates unbound to membrane remain at the bottom of the gradient (Ono and Freed, 1999; Spearman et al., 1997; Swanson and Hoppe, 2004). When the distribution of ectopically expressed HA-Dvl-2-EGFP was analysed in this manner, although a small proportion of HA-Dvl-2-GFP was found in the membrane-associated fractions, the majority of the protein partitioned in the bottom fraction supporting the notion that ectopically expressed HA-Dvl-2-GFP formed membrane-free protein aggregates. A previous study using a similar approach also concluded that endogenous Dvl was cytosolic and did not co-segregate with membrane fractions (Reinacher-Schick and Gumbiner, 2001).

Discussion

We have investigated the nature and the significance of the ‘vesicular’ distribution of exogenously expressed Dvl-2 protein

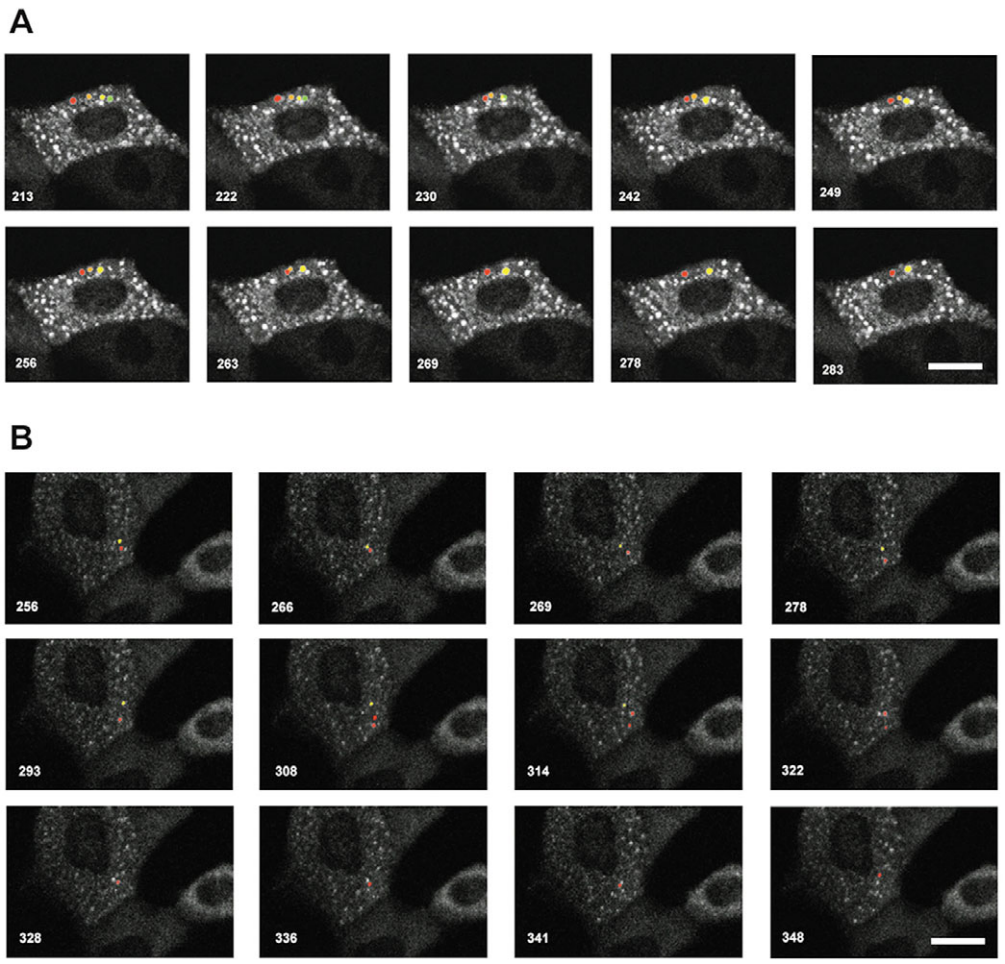

Fig. 7. Time-lapse analysis of HA-Dvl-2-EGFP puncta. (A) Still frames from Movie 1B in supplementary material, illustrating lack of coordinated or directional movement in fluorescent bodies in a cell ectopically expressing HA-Dvl-2-EGFP at high levels. Frame numbers are indicated. Four bodies are false-coloured in the first frame (213) so that their fate may be followed. Note the yellow and green bodies fuse in frame 230 and the orange and red bodies fuse via a ‘dumb-bell’ intermediate in frame 263. (B) Still frames from Movie 1C in supplementary material, illustrating lack of coordinated or directional movement in fluorescent bodies in a cell expressing lower levels of HA-Dvl-2-EGFP. Frame numbers are indicated. Two bodies are false coloured in the first frame (256) so that their fate may be followed. Note the red body appeared to split into two between frames 293 and 308, the yellow body disappeared by frame 314 and one of the two bodies resulting from the split of the red body disappeared by frame 328. Bars, 12 μm.

that many authors, including ourselves, have reported (Axelrod et al., 1998; Cliffe et al., 2003; Fagotto et al., 1999; Smalley et al., 1999; Torres and Nelson, 2000). We have established a number of key points. First, the predominant staining pattern in transiently ectopically expressed Dvl-2, whether in its EGFP-fusion constitutively active form or its ER-fusion inducible form, is in cytoplasmic puncta, as previously observed. By contrast, very low levels of expression resulted in localisation at the MTOC and in a juxtamembrane region near the cortical actin cytoskeleton. Second, formation of visible puncta following high-level transient ectopic expression is dependent upon the DIX domain and independent of the PDZ domain, but activation of the canonical Wnt pathway in this situation is dependent on both the DIX and PDZ domains. Localisation at, or formation of, these structures is therefore not sufficient for pathway activation. Third, at single-copy expression levels, β-catenin accumulation occurs without punctate body formation and with the same time course as Dvl-2 relocalisation to the MTOC and the juxtamembrane region following β-estradiol activation. Thus, Dvl-2-dependent canonical Wnt pathway activation can occur when Dvl-2 is distributed in either of the two localisation patterns described. Fourth, the punctate Dvl-2 bodies do not seem to be related to an endocytic compartment as they failed to colocalise with any markers of the endocytic pathways or to affect the distribution of these markers and the appearance of early and late endosomes in Dvl-2 expressing cells (data not shown). Fifth, Dvl-2 puncta are not membrane-bound as assessed by EM. Finally, time-lapse analysis indicated that the punctate structures were not generated by endocytosis as they did not appear to originate from the plasma membrane or traffic directionally from the periphery of the cell. Furthermore, our measurements of the velocity of the smaller puncta (0.024±0.01 μm/second) indicated that they travelled relatively slowly, compared with, for instance, velocities previously reported for microtubule-associated transport, e.g. from 0.6 to 2.0 μm/second (Bohm et al., 2000) and 2.4 μm/second reported in axons (Hasaka et al., 2004). They also travel more slowly than 'vesicular structures' containing c-kit fusion proteins ectopically expressed in COS cells (Jahn et al., 2002) that moved in guided, radial tracks from the periphery to the centre of the cell, and vice versa. In this system, this directional speed of travel was measured at 0.05 to 0.2 μm/second (Jahn et al., 2002).

These data strongly suggest that the predominant Dvl-2 localisation pattern following ectopic expression at high levels, namely puncta, is not a physiological signalling compartment. We suggest, rather, that these are protein aggregates. However, high level Dvl-2 ectopic expression does activate canonical Wnt signalling (Fig. 3) (Smalley et al., 1999). The mechanism for this is unclear. We have previously demonstrated that ectopic expression of HA-Dvl-2 carrying a membrane localisation motif (CAAX box) causes relocalisation of coexpressed FLAG-tagged axin from a cytoplasmic compartment to the cell membrane (Smalley et al., 1999). Conversely, ectopic expression of an epitope-tagged axin construct caused coexpressed Dishevelled to relocate from cytoplasmic puncta to the cell membrane (Fagotto et al., 1999). This is evidence of an extremely strong interaction between these proteins. We therefore suggest that the DIX domain-dependent interaction of Dvl-2 with axin results in endogenous axin also being incorporated into the protein aggregates. This would disrupt the function of the β-catenin turnover complex, allowing β-catenin to accumulate and activating TCF-dependent transcription. Of course, we cannot exclude the possibility that sequestering of axin into inactive protein aggregates may underly β-catenin stabilisation in the single-copy cell line, or could even be involved in physiological ligand-dependent signalling.

In addition to the punctate structures, juxtamembrane and MTOC localisation described here, Dishevelled has also been reported in association with actin, microtubules and the nucleus (Capelluto et al., 2002; Ciani et al., 2004; Habas and Dawid, 2005; Itoh et al., 2005; Krylova et al., 2000; Torres and Nelson, 2000). Our data support an interaction with the MTOC and a partial microtubule-dependency on localisation, at least at low expression levels. In future, the wider availability of high-quality anti-Dishevelled reagents that have been validated against systems lacking the cognate proteins should help validate and confirm the functional importance of particular intracellular Dishevelled pools of protein.

The data we have presented here have demonstrated that canonical Wnt signalling can occur in the absence of the formation of Dvl-2 cytoplasmic puncta and that the appearance of these bodies following ectopic expression is likely to be due to DIX-domain-dependent protein aggregation. These data will help in the understanding of the role of Dishevelled in Wnt signalling.

The authors thank Professor Tariq Enver for his gift of the EFG2ERP plasmid and Jonathan Franca-Koh, Keith Wu and Elizabeth Frazer for technical support. This work was supported by Cancer Research UK, Breakthrough Breast Cancer and The Medical Research Council.

References

Axelrod, J. D., Miller, J. R., Shulman, J. M., Moon, R. T. and Perrimon, N. (1998). Differential recruitment of Dishevelled provides signaling specificity in the planar cell polarity and Wingless signaling pathways. *Genes Dev.* **12**, 2610-2622.

Bejsovec, A. (2005). Wnt pathway activation: new relations and locations. *Cell* **120**, 11-14.

Bohm, K. J., Stracke, R. and Unger, E. (2000). Speeding up kinesin-driven microtubule gliding in vitro by variation of cofactor composition and physicochemical parameters. *Cell Biol. Int.* **24**, 335-341.

Boutros, M. and Mlodzik, M. (1999). Dishevelled: at the crossroads of divergent intracellular signaling pathways. *Mech. Dev.* **83**, 27-37.

Boutros, M., Paricio, N., Strutt, D. I. and Mlodzik, M. (1998). Dishevelled activates JNK and discriminates between JNK pathways in planar polarity and wingless signaling. *Cell* **94**, 109-118.

Carlemalm, E., Garavito, R. M. and Villinger, W. (1982). Resin development for electron microscopy and an analysis of embedding at low termperature *J. Microsc.* **126**, 123-143.

Capelluto, D. G., Kutateladze, T. G., Habas, R., Finkielstein, C. V., He, X. and Overduin, M. (2002). The DIX domain targets dishevelled to actin stress fibres and vesicular membranes. *Nature* **419**, 726-729.

Chen, W., ten Berge, D., Brown, J., Ahn, S., Hu, L. A., Miller, W. E., Caron, M. G., Barak, L. S., Nusse, R. and Lefkowitz, R. J. (2003). Dishevelled 2 recruits β-arrestin 2 to mediate Wnt5A-stimulated endocytosis of Frizzled 4. *Science* **301**, 1391-1394.

Choi, S. C. and Han, J. K. (2005). Rap2 is required for Wnt/β-catenin signaling pathway in Xenopus early development. *EMBO J.* **24**, 985-996.

Ciani, L., Krylova, O., Smalley, M. J., Dale, T. C. and Salinas, P. C. (2004). A divergent canonical WNT-signaling pathway regulates microtubule dynamics: dishevelled signals locally to stabilize microtubules. *J. Cell Biol.* **164**, 243-253.

Cliffe, A., Hamada, F. and Bienz, M. (2003). A role of Dishevelled in

relocating Axin to the plasma membrane during wingless signaling. *Curr. Biol.* **13**, 960-966.

Cong, F. and Varmus, H. (2004). Nuclear-cytoplasmic shuttling of Axin regulates subcellular localization of β-catenin. *Proc. Natl. Acad. Sci. USA* **101**, 2882-2887.

Cong, F., Schweizer, L. and Varmus, H. (2004). Wnt signals across the plasma membrane to activate the β-catenin pathway by forming oligomers containing its receptors, Frizzled and LRP. *Development* **131**, 5103-5115.

Ding, V. W., Chen, R. H. and McCormick, F. (2000). Differential regulation of glycogen synthase kinase 3β by insulin and Wnt signaling. *J. Biol. Chem.* **275**, 32475-32481.

Dubois, L., Lecourtois, M., Alexandre, C., Hirst, E. and Vincent, J. P. (2001). Regulated endocytic routing modulates wingless signaling in Drosophila embryos. *Cell* **105**, 613-624.

Fagotto, F., Jho, E., Zeng, L., Kurth, T., Joos, T., Kaufmann, C. and Costantini, F. (1999). Domains of axin involved in protein-protein interactions, Wnt pathway inhibition, and intracellular localization. *J. Cell Biol.* **145**, 741-756.

Fraile-Ramos, A., Kledal, T. N., Pelchen-Matthews, A., Bowers, K., Schwartz, T. W. and Marsh, M. (2001). The human cytomegalovirus US28 protein is located in endocytic vesicles and undergoes constitutive endocytosis and recycling. *Mol. Biol. Cell* **12**, 1737-1749.

Habas, R. and Dawid, I. B. (2005). Dishevelled and Wnt signaling: is the nucleus the final frontier? *J. Biol.* **4**, DOI 10.1186.

Hasaka, T. P., Myers, K. A. and Baas, P. W. (2004). Role of actin filaments in the axonal transport of microtubules. *J. Neurosci.* **24**, 11291-11301.

Heisenberg, C. P., Tada, M., Rauch, G. J., Saude, L., Concha, M. L., Geisler, R., Stemple, D. L., Smith, J. C. and Wilson, S. W. (2000). Silberblick/Wnt11 mediates convergent extension movements during zebrafish gastrulation. *Nature* **405**, 76-81.

Itoh, K., Brott, B. K., Bae, G. U., Ratcliffe, M. J. and Sokol, S. Y. (2005). Nuclear localization is required for Dishevelled function in Wnt/β-catenin signaling. *J. Biol.* **4**, DOI 10.1186.

Jahn, T., Seipel, P., Coutinho, S., Urschel, S., Schwarz, K., Miething, C., Serve, H., Peschel, C. and Duyster, J. (2002). Analysing c-kit internalization using a functional c-kit-EGFP chimera containing the fluorochrome within the extracellular domain. *Oncogene* **21**, 4508-4520.

Johnston, J. A., Ward, C. L. and Kopito, R. R. (1998). Aggresomes: a cellular response to misfolded proteins. *J. Cell Biol.* **143**, 1883-1898.

Kishida, S., Yamamoto, H., Hino, S., Ikeda, S., Kishida, M. and Kikuchi, A. (1999). DIX domains of Dvl and axin are necessary for protein interactions and their ability to regulate β-catenin stability. *Mol. Cell. Biol.* **19**, 4414-4422.

Klingensmith, J., Nusse, R. and Perrimon, N. (1994). The Drosophila segment polarity gene dishevelled encodes a novel protein required for response to the wingless signal. *Genes Dev.* **8**, 118-130.

Korinek, V., Barker, N., Morin, P. J., van Wichen, D., de Weger, R., Kinzler, K. W., Vogelstein, B. and Clevers, H. (1997). Constitutive transcriptional activation by a β-catenin-Tcf complex in APC–/– colon carcinoma. *Science* **275**, 1784-1787.

Krylova, O., Messenger, M. J. and Salinas, P. C. (2000). Dishevelled-1 regulates microtubule stability: a new function mediated by glycogen synthase kinase-3β. *J. Cell Biol.* **151**, 83-94.

Kuhl, M., Sheldahl, L. C., Park, M., Miller, J. R. and Moon, R. T. (2000). The Wnt/Ca2+ pathway: a new vertebrate Wnt signaling pathway takes shape. *Trends Genet.* **16**, 279-283.

Le Roy, C. and Wrana, J. L. (2005). Clathrin- and non-clathrin-mediated endocytic regulation of cell signalling. *Nat. Rev. Mol. Cell. Biol.* **6**, 112-126.

Li, L., Yuan, H., Xie, W., Mao, J., Caruso, A. M., McMahon, A., Sussman, D. J. and Wu, D. (1999). Dishevelled proteins lead to two signaling pathways. Regulation of LEF-1 and c-Jun N-terminal kinase in mammalian cells. *J. Biol. Chem.* **274**, 129-134.

Mao, B., Wu, W., Li, Y., Hoppe, D., Stannek, P., Glinka, A. and Niehrs, C. (2001). LDL-receptor-related protein 6 is a receptor for Dickkopf proteins. *Nature* **411**, 321-325.

Miller, J. R., Hocking, A. M., Brown, J. D. and Moon, R. T. (1999). Mechanism and function of signal transduction by the Wnt/β-catenin and Wnt/Ca2+ pathways. *Oncogene* **18**, 7860-7872.

Moon, R. T. (2005a). Wnt/β-catenin pathway. *Sci. STKE* **2005**, cm1.

Moon, R. T. (2005b). Xenopus egg Wnt/β-catenin pathway. *Sci. STKE* **2005**, cm2.

Moriguchi, T., Kawachi, K., Kamakura, S., Masuyama, N., Yamanaka, H., Matsumoto, K., Kikuchi, A. and Nishida, E. (1999). Distinct domains of mouse dishevelled are responsible for the c-Jun N-terminal kinase/stress-activated protein kinase activation and the axis formation in vertebrates. *J. Biol. Chem.* **274**, 30957-30962.

Nagahata, T., Shimada, T., Harada, A., Nagai, H., Onda, M., Yokoyama, S., Shiba, T., Jin, E., Kawanami, O. and Emi, M. (2003). Amplification, up-regulation and over-expression of DVL-1, the human counterpart of the Drosophila disheveled gene, in primary breast cancers. *Cancer Sci.* **94**, 515-518.

Okino, K., Nagai, H., Hatta, M., Nagahata, T., Yoneyama, K., Ohta, Y., Jin, E., Kawanami, O., Araki, T. and Emi, M. (2003). Up-regulation and overproduction of DVL-1, the human counterpart of the Drosophila dishevelled gene, in cervical squamous cell carcinoma. *Oncol. Rep.* **10**, 1219-1223.

Ono, A. and Freed, E. O. (1999). Binding of human immunodeficiency virus type 1 Gag to membrane: role of the matrix amino terminus. *J. Virol.* **73**, 4136-4144.

Reinacher-Schick, A. and Gumbiner, B. M. (2001). Apical membrane localization of the adenomatous polyposis coli tumor suppressor protein and subcellular distribution of the β-catenin destruction complex in polarized epithelial cells. *J. Cell Biol.* **152**, 491-502.

Rothbacher, U., Laurent, M. N., Deardorff, M. A., Klein, P. S., Cho, K. W. and Fraser, S. E. (2000). Dishevelled phosphorylation, subcellular localization and multimerization regulate its role in early embryogenesis. *EMBO J.* **19**, 1010-1022.

Signoret, N. and Marsh, M. (2000). Analysis of chemokine receptor endocytosis and recycling. *Methods Mol. Biol.* **138**, 197-207.

Signoret, N., Pelchen-Matthews, A., Mack, M., Proudfoot, A. E. and Marsh, M. (2000). Endocytosis and recycling of the HIV coreceptor CCR5. *J. Cell Biol.* **151**, 1281-1294.

Signoret, N., Hewlett, L., Wavre, S., Pelchen-Matthews, A., Oppermann, M. and Marsh, M. (2005). Agonist-induced endocytosis of CC chemokine receptor 5 is clathrin dependent. *Mol. Biol. Cell* **16**, 902-917.

Smalley, M. J. and Dale, T. C. (2001). Wnt signaling and mammary tumorigenesis. *J. Mammary Gland Biol. Neoplasia* **6**, 37-52.

Smalley, M. J., Titley, J. and O'Hare, M. J. (1998). Clonal characterization of mouse mammary luminal epithelial and myoepithelial cells separated by fluorescence-activated cell sorting. *In Vitro Cell Dev. Biol. Anim.* **34**, 711-721.

Smalley, M. J., Sara, E., Paterson, H., Naylor, S., Cook, D., Jayatilake, H., Fryer, L. G., Hutchinson, L., Fry, M. J. and Dale, T. C. (1999). Interaction of axin and Dvl-2 proteins regulates Dvl-2-stimulated TCF-dependent transcription. *EMBO J.* **18**, 2823-2835.

Sokol, S. Y. (1996). Analysis of Dishevelled signalling pathways during Xenopus development. *Curr. Biol.* **6**, 1456-1467.

Spearman, P., Horton, R., Ratner, L. and Kuli-Zade, I. (1997). Membrane binding of human immunodeficiency virus type 1 matrix protein in vivo supports a conformational myristyl switch mechanism. *J. Virol.* **71**, 6582-6592.

Sussman, D. J., Klingensmith, J., Salinas, P., Adams, P. S., Nusse, R. and Perrimon, N. (1994). Isolation and characterization of a mouse homolog of the Drosophila segment polarity gene dishevelled. *Dev. Biol.* **166**, 73-86.

Swanson, J. A. and Hoppe, A. D. (2004). The coordination of signaling during Fc receptor-mediated phagocytosis. *J. Leukoc. Biol.* **76**, 1093-1103.

Tamai, K., Semenov, M., Kato, Y., Spokony, R., Liu, C., Katsuyama, Y., Hess, F., Saint-Jeannet, J. P. and He, X. (2000). LDL-receptor-related proteins in Wnt signal transduction. *Nature* **407**, 530-535.

Theisen, H., Purcell, J., Bennett, M., Kansagara, D., Syed, A. and Marsh, J. L. (1994). dishevelled is required during wingless signaling to establish both cell polarity and cell identity. *Development* **120**, 347-360.

Tolwinski, N. S., Wehrli, M., Rives, A., Erdeniz, N., DiNardo, S. and Wieschaus, E. (2003). Wg/Wnt signal can be transmitted through arrow/LRP5,6 and Axin independently of Zw3/Gsk3β activity. *Dev. Cell* **4**, 407-418.

Torres, M. A. and Nelson, W. J. (2000). Colocalization and redistribution of dishevelled and actin during Wnt-induced mesenchymal morphogenesis. *J. Cell Biol.* **149**, 1433-1442.

Wallingford, J. B., Rowning, B. A., Vogeli, K. M., Rothbacher, U., Fraser, S. E. and Harland, R. M. (2000). Dishevelled controls cell polarity during Xenopus gastrulation. *Nature* **405**, 81-85.

Wu, J., Yang, J. and Klein, P. S. (2005). Neural crest induction by the canonical Wnt pathway can be dissociated from anterior-posterior neural patterning in Xenopus. *Dev. Biol.* **279**, 220-232.

Zhang, Y., Neo, S. Y., Han, J. and Lin, S. C. (2000). Dimerization choices control the ability of axin and dishevelled to activate c-Jun N-terminal kinase/stress-activated protein kinase. *J. Biol. Chem.* **275**, 25008-25014.

Journal of Cell Science